This article has been accepted for publication in a future issue of this journal, but has not been fully edited. Content may change prior to final publication. Citation information: DOI 10.1109/TPWRD.2018.2834138, IEEE Transactions on Power Delivery

Simulation of Switching Overvoltages and Validation with Field Tests

IEEE-PES Working Group on Field Measured Overvoltages and Their Analysis
Chairman: Reynaldo Ramos Vice-Chair: Ilhan Kocar Secretary: Alejandro Montenegro

Contributors: M. Cervantes, *Student Member, IEEE,* I. Kocar, *Senior Member, IEEE,* A. Montenegro, *Member, IEEE,* D. Goldsworthy, *Senior Member, IEEE,* T. Tobin, *Fellow, IEEE,* J. Mahseredjian, *Fellow, IEEE,* R. Ramos, *Senior Member, IEEE, J. Marti, Fellow, IEEE,* T. Noda, *Senior Member, IEEE,* A. Ametani, *Life Fellow, IEEE,* C. Martin, *Member, IEEE*

***Abstract*— On transmission lines where switching surges are not mitigated with closing resistors and/or surge arresters, high-speed reclosing on a line with trapped charge will produce high overvoltages that have been measured above 3 pu. Careful simulations of these switching events using available Electromagnetic Transient (EMT) programs consistently produce significantly higher voltages than the measurements. This indicates a phenomenon present on the line that acts to reduce the switching surge magnitudes but is not typically modeled. This paper aims to identify the required simulation practices in reproducing the field measured overvoltages in EMT simulations and investigates the sensitivity of results to modeling approaches and electrical parameters. Field measurements from a switching surge test of a 230-kV line without surge mitigation have been used for model comparisons. Variations in frequency-dependent line modeling, ground resistivity, skin effect, shunt conductance, parallel lines and source-side detail have been tested in an unsuccessful attempt to decrease the difference between the field measurements and the higher simulation overvoltages. It is demonstrated that even though the pattern of the transient voltage waveforms can be reproduced very well using frequency-dependent line models, the magnitude of the maximum overvoltage is significantly overestimated unless the effect of corona is considered. Two types of corona models are tested, and both demonstrate that corona is the primary factor that allows the simulations to correctly reproduce high peak overvoltage measurements.**

M. Cervantes, I. Kocar, J. Mahseredjian, and A. Ametani are with Polytechnique Montréal, Montreal, QC H3T 1J4, Canada (e-mail: miguel.cervantes-martinez@polymtl.ca; ilhan.kocar@polymtl.ca; jean.mahseredjian@polymtl.ca; aametani@mail.doshisha.ac.jp).

A. Montenegro and T. Tobin are with S&C Electric Company, Chicago, IL 60626, USA (e-mail: Alejandro.Montenegro@sandc.com; Tom.Tobin @sandc.com).

D. Goldsworthy and C. Martin are with Bonneville Power Administration (BPA), Portland, OR 97232, USA (e-mail: dlgoldsworthy@bpa.gov; cjmartin@bpa.gov).

R. Ramos is with Southern Company Services Transmission Planning, Birmingham, AL, USA (e-mail: rramos@southernco.com).

J. Marti is with the Department of Electrical and Computer Engineering, University of British Columbia, Vancouver, BC V6T 1Z4, Canada (e-mail: jrms@ece.ubc.ca).

T. Noda is with the Electric Power Engineering Research Laboratory, Central Research Institute of Electric Power Industry (CRIEPI), Kanagawa 240-0196, Japan (e-mail: takunoda@criepi.denken.or.jp).

***Index Terms*—Corona, frequency dependent line models, field measurements, switching transients, transmission lines, EMT-type programs**

I. Introduction

Switching of transmission lines results in electromagnetic transients that propagate along the lines as discussed in many references, among others [1]-[4]. The switching overvoltages are more significant during high-speed reclosing due to the trapped charge on the line [5]. Switching overvoltages tend to be well controlled at the extra high voltage (EHV) level with closing resistors and/or arresters, but below that level they have not historically been controlled. Although arresters are common today, older lines used rod gaps installed at the ends of the line to protect the substation equipment by flashing over during lightning overvoltages. However, below EHV switching overvoltages may also be sufficiently high to flash over the rod gaps during high-speed line reclosing. Such an event occurred on the Bonneville Power Administration (BPA) Big Eddy-Chemawa 230 kV line and prompted an investigation and switching surge field test as describe in [6]-[7].

The 1995 field test performed by BPA was intended to verify the modeling techniques in Electromagnetic Transient-type (EMT-type) Programs, and determine the highest overvoltages at the receiving end of a 230-kV line during high-speed reclosing with a trapped charge [7]. The resulting measurements included data taken at 1 MHz for 50 high-speed reclosing tests with a maximum measured overvoltage of 3.3 pu. The first paper of the work group [6] provides a description of the BPA field test, including the purpose, procedures and measurements along with a summary of the main results. The recorded field measurements provide a unique opportunity for the experimental validation of line models [8]-[10] at high overvoltage levels in EMT-type programs.

Rather than validate the EMT studies as hoped, the field measurements actually showed that for the highest switching surge voltage levels, the EMT studies are not accurate and overestimate the overvoltages by about 1 pu, or 30%.

This article has been accepted for publication in a future issue of this journal, but has not been fully edited. Content may change prior to final publication. Citation information: DOI 10.1109/TPWRD.2018.2834138, IEEE Transactions on Power Delivery

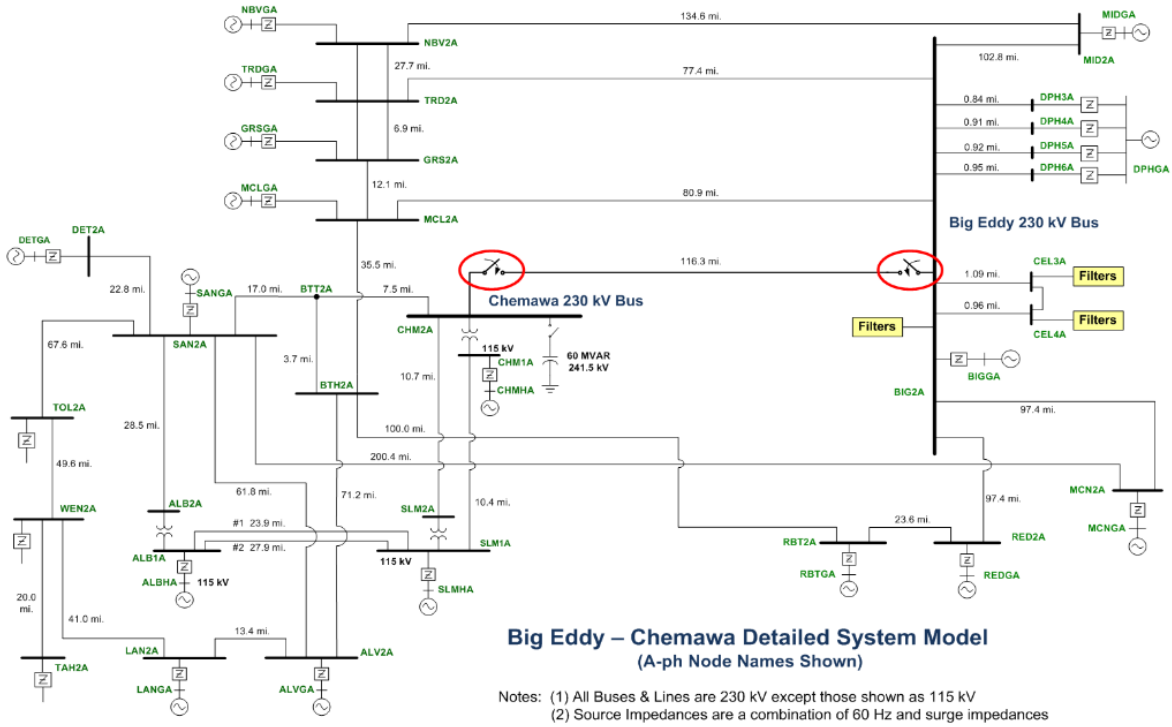

Fig. 1. Big Eddy-Chemawa 230-kV detailed system model, [17].

Specifically, statistical switching surge simulations for this same 230 kV line predict overvoltages in excess of 4.3 pu, where the highest overvoltages measured were 3.3 pu.

The importance of this becomes clear when it is recalled that the highest 2% of overvoltage results of switching surge studies are normally used for line design and reliability purposes, while the maximum overvoltages are often used for safety-related purposes such as minimum approach distances. The work described in this paper is therefore focused on those highest measured overvoltages and what can be done to close the gap between measurements and simulations and bring more accuracy to these switching surge studies.

The reader is reminded that this work is not targeted toward the situations where switching surges are controlled to lower levels by the use of surge arresters, closing resistors or where trapped charge is removed prior to closing. For those situations the overvoltages are lower and EMT programs, using standard modeling techniques, are considerably more accurate. For the unique case of shunt-compensated lines, the high overvoltages can still occur where the reactor and accompanying surge arrester are on the same end of the line as the first breaker to reclose.

The objectives of this second paper are to understand the major factors in the reproduction of field measurements using simulations and to investigate the sensitivity of simulations to various modeling and electrical parameters. For validation purposes, the waveforms recorded during the "*Three-phase line switching test series*" reported in [7] are used since they approximate high-speed reclosing and produced the highest switching-surge overvoltages. In principle, once a line model is validated, it is possible to proceed with statistical simulation phase to identify the worst-case overvoltage, which is of utmost importance for transmission line and substation related issues such as the evaluation of minimum approach distance and clearance practices [7].

According to the simulation studies presented in this paper, refinements in ground resistivity, skin effect, phase-to-ground conductance and detailed source modeling are not sufficient to match maximum transient overvoltages. The peak of the transient voltage is significantly overestimated unless the effect of corona is included. It is recalled here that the line under test is not equipped with arrestors, and no closing resistors are used in switching. On the other hand, the pattern of the transient overvoltage waveforms is matched when frequency dependent line models are employed and multiple prestrikes during reclosure of the breaker are sequentially produced in the simulation environment.

The representation of corona involves a distributed nonlinear hysteresis behavior, and it is complex to combine it with the line model equations in EMT studies [11]-[15]. Most of the methods proposed in the literature rely on subdividing the line into linear subsections and represent corona with non-linear shunt branches at each junction [14]. In this paper, the Suliciu Model [13] and the linear corona model [16] are used. Both models require subdividing the line into linear sections.

The paper is structured as follows: The test system and the study cases are introduced in Section II. Modeling details and parameters of the test system are given in Section III. Preliminary simulation results are presented in Section IV. The sensitivity of simulation results to modeling parameters is analyzed in Section V. Section VI shows the results by considering the corona effect using two different corona models. Additional study cases are presented in Section VII to demonstrate the performance of corona model for other test cases.

II. Big Eddy-Chemawa Test System

The Big Eddy-Chemawa line is a 230-kV line of 116 miles long. It originates at the Big Eddy Substation near The Dalles, Oregon, and terminates at the Chemawa Substation near Salem, Oregon. Fig. 1 shows the one-line diagram of the Big Eddy-Chemawa 230-kV line and the detailed test system. The results of the BPA field investigation are reported in [7]. The BPA report includes overvoltage and field data recorded during the switching surge field test on the Big Eddy-Chemawa line. The switching surge field tests consist of single-phase and three-phase line switching with and without trapped charge. The three-phase test is selected in this paper since it produced the highest overvoltages [7].

A. Three-phase Line Switching Test (Test Series 5)

The purpose of the three-phase test was the collection of measurements for the verification of EMT models and statistical data on overvoltages that could be expected during high-speed reclosing [7]. The highest switching surge overvoltage occurs when reclosing a line with trapped charge. In Test Series 5 reported in [7], switch opening was controlled and synchronized to generate the same polarity and magnitude of trapped charge on each phase for each of the reclosing tests. The breaker closing times were varied uniformly over a complete 60 Hz cycle by increments of 18 electrical degrees (1/20 cycle). Closing from Big Eddy provided line switching measurements with a strong source, while closing from Chemawa provided measurements with a relatively weak source. This paper includes mainly the switching transient analysis for the cases 5-02, 5-03, 5-05 (switching from Big Eddy side), and 5-53 (switching from Chemawa side) of [7] since they present the highest overvoltage levels. The overvoltages measured at each end of the line during these cases are listed in Table I, whereas the trapped charge values are presented in Table II. The steady-state peak line-to-ground bus voltage prior to switching was 197.6 kV at Big Eddy and 187.4 kV at Chemawa.

TABLE I
THREE-PHASE LINE SWITCHING, PEAK VOLTAGES (KV)

Case	Big Eddy end line voltage			Chemawa end line voltage		
	A-Ph	B-Ph	C-Ph	A-Ph	B-Ph	C-Ph
5-02	442.3	-284.1	-493.8	505.6	445.9	-643.2
5-03	452.1	409.9	-570.6	566.6	561.6	-638.9
5-05	459.7	-284.0	-541.9	536.9	529.2	-622.8
5-53	-587.0	-569.8	497.4	-394.4	332.5	288.9

TABLE II
TRAPPED CHARGE VOLTAGES (KV)

Case	Φ*	A-Ph	B-Ph	C-Ph
5-02	0	-235.4	-176.4	179.6
5-03	18	-230.9	-175.2	179.8
5-05	54	-234.3	-177.4	181.9
5-53	18	221.2	185.1	-184.14

*Relative closing angle in degrees.

B. Field Test Data

The critical line voltage measurements were made with laboratory-quality RCR dividers to ensure accurate measurements from dc to 1 MHz as described in the first paper of the WG [6].

III. Test System Modeling in EMTP

To reproduce the field measurements using simulations, the test system is modeled with varying level of details. Line parameters, conductor data and other relevant system details are given in [7] and [17]. A description of the various modeling approaches and details used in this paper is presented below.

A. Big Eddy-Chemawa Line Model

As shown in the right-of-way drawing of Fig. 3, there are two additional 230-kV lines parallel to the Big Eddy-Chemawa line for part of its length, along with a 525-kV line.

In this paper, the Big Eddy-Chemawa line is modeled together with the three parallel lines due to their impact on transients as will be shown in Section V-A. The configuration of this line system, consisting of 10 sections with different geometry, is illustrated in Fig. 3. All the sections are modeled using either the wideband (WB) model which is the implementation of the Universal Line Model in EMTP [8], the frequency-dependent (FD) line model [9], and the constant parameters (CP) model [10]. The line parameters including conductor data and line geometries at different sections are available in [17]. The CP model parameters are evaluated at 1 and 10 kHz.

B. Trapped Charge Model

To account for the trapped charge on the line, a three-phase dc voltage source is connected to the line with magnitudes as given in Table II. The source is disconnected at the instant when the switching transients are triggered.

C. Filter and Capacitor Bank Models

Filters and capacitor banks seen in Fig. 1 are modeled with equivalent circuits. The equivalent models connected at the Chemawa and Big Eddy buses are shown in Fig. 2 with the numerical parameters of the components [17].

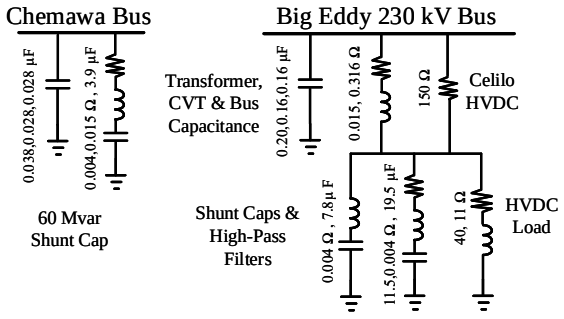

Fig. 2. Equivalent model for filters and capacitor banks

This article has been accepted for publication in a future issue of this journal, but has not been fully edited. Content may change prior to final publication. Citation information: DOI 10.1109/TPWRD.2018.2834138, IEEE Transactions on Power Delivery

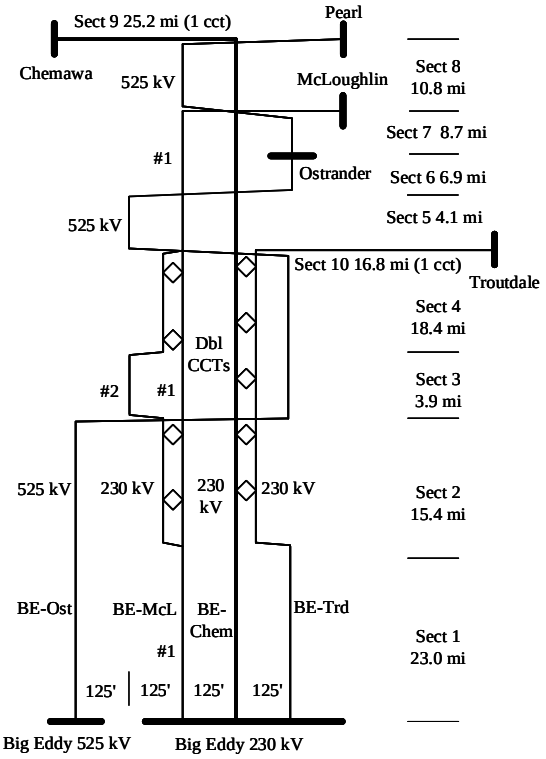

Fig. 3. One-line diagram of Big Eddy-Chemawa and parallel lines, [17].

D. Simplified and Detailed Source Models

The surrounding system connected to the Big Eddy-Chemawa line and its parallel lines, is either represented by using simplified equivalent source models as shown in Fig. 4 or the detailed source model, i.e. with surrounding system, as given in Fig. 1. The source and surge impedance data is listed in Table III for the simplified source models (subscript 1 and 0 stand for positive and zero sequence, respectively). Table IV shows the bus voltage levels used in the simulations. The angles are initialized through steady state solution.

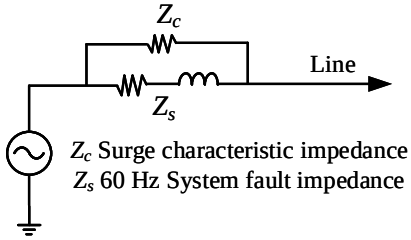

Fig. 4. Simplified source model, [17].

TABLE III
SOURCE IMPEDANCE DATA FOR BUSES ALONG BIG EDDY-CHEMAWA LINE

Bus	Z_s (Ω)				Z_c (Ω)	
	R_1	X_1	R_0	X_0	Zc_1	Zc_0
Big Eddy 230	0.12	3.1	0.06	2.0	42	81
Chemawa	1.60	12.6	1.30	16.0	190	365
McLoughlin	0.28	4.8	0.24	4.1	63	122
Troutdale	0.36	5.0	0.31	4.8	76	146
Big Eddy 525	0.70	14.0	0.60	12.0	56	130
Ostrander	1.80	21.0	2.20	25.0	93	217
Pearl	1.30	20.0	2.10	24.0	140	325

TABLE IV
SOURCE VOLTAGE DATA FOR BUSES ALONG BIG EDDY-CHEMAWA LINE

Bus	Nominal voltage (kV)	Approximated bus Voltage (kV)	Voltage angle phase A (deg)
Big Eddy 230	230	240	0
Chemawa	230	237	0
McLoughlin	230	238	-11
Troutdale	230	238	-11.7
Big Eddy 525	525	542	0
Ostrander	525	539	-4.5
Pearl	525	539	-10

E. Prestrike Modeling

There are multiple prestrikes during the closing events, as described in [6], and they are different for each phase. The switching times are very important for producing the exact waveform of transients [5]. The multiple prestrikes are modeled by a set of switches, which is connected at the sending end of the line. The switch closing times are determined from the voltage and current measurements. The opening time is the first instant when the current crosses zero during the transients. Forcing the interruption at an instant determined from the measurements alone generates current chopping phenomenon that mismatches the pattern of field measurements in simulations. The sequence of switching times is given in the Appendix.

F. Tabulated Source Model

As an alternative to the modeling of prestrikes, a tabulated source using the measurements at the switching end is also tested. In this case the source is an ideal source that forces the measurements at the sending end of the line. This approach is supposed to account for the impact of prestrikes intrinsically.

IV. PRELIMINARY SWITCHING TRANSIENT STUDIES

This section is the initial study step on the field test results of Case 5-03. The system of parallel lines in Fig. 3 is built by considering the modeling approaches described in Section III. Two cases are studied for the energization of the Big Eddy-Chemawa line system:

1) Tabulated source model using measurements
2) Simplified source using switches for prestrikes

To simplify the comparisons between waveforms, only one phase with substantial overvoltages will be shown.

A. Tabulated Source Model

In this case, the Big Eddy-Chemawa line model is energized at the Big Eddy end by a tabulated source. The voltage of phase A at the Chemawa end is shown in Fig. 5. The different line models, including FD, WB, and CP are compared with the field data. Note the -231 kV initial trapped charge in the measurements and on the line models. Fig. 5 shows that the WB and FD models yield similar results. But they don't follow the pattern of the field data, there are unexpected spikes, and there is a mismatch of 0.23 pu in peak values compared to the measured value of 3.02 pu. The damping in simulations seems to be slower than the one in measurements, which may be due to the lack of surge impedance in the tabulated source. On the other hand, Fig. 5 shows that the

This article has been accepted for publication in a future issue of this journal, but has not been fully edited. Content may change prior to final publication. Citation information: DOI 10.1109/TPWRD.2018.2834138, IEEE Transactions on Power Delivery

waveform associated with the CP model is not as accurate as the ones obtained with the FD or WB model. The performance of the CP model depends on the frequency at which the parameters are evaluated. In the cases of Fig. 5 and Fig. 6, 1 kHz provides better results than 10 kHz.

Adjustments in ground resistivity and phase to ground conductances did not improve the results significantly (not shown).

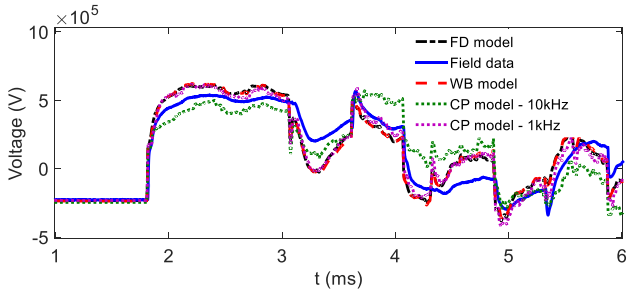

Fig. 5. Voltage of phase A at Chemawa end, tabulated source model.

B. *Simplified Source Model with Prestrike*

In this test, the Big Eddy-Chemawa line is energized from the Big Eddy bus using a simplified source with prestrikes created with a set of switches as described in Section III-E. The voltage of phase A at the Chemawa end for the simplified source model is shown in Fig. 6. It can be observed in Fig. 6 that the WB and FD models produce simulation results that are very close to each other. However, although the voltage waveforms follow the pattern of the field measurements better compared to the previous test case, the peak voltages are overestimated by about 1.62 pu. On the other hand, as in the previous test case, the CP model does not follow the waveform pattern. It is noted that the frequency dependence of line parameters is important in this study.

Similar results are obtained with different ground resistivity and different phase to ground conductance values (not shown).

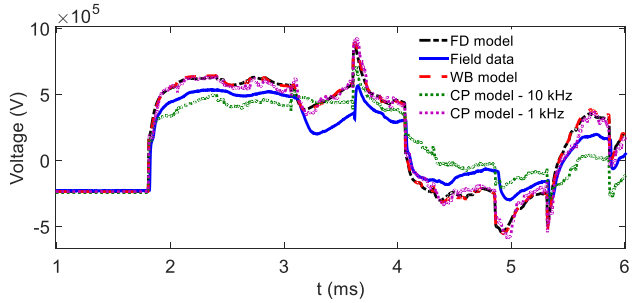

Fig. 6. Voltage of phase A at Chemawa end, simplified source model.

C. *Comparison of Tabulated and Simplified Source Models*

Modeling the Big Eddy-Chemawa line system by using the FD model only, a comparison between the results of tabulated and simplified source model is presented in Fig. 7. The simplified source model produces waveforms that follow the field data better but overestimates the peak more than the tabulated source model does.

An analysis on the line parameters is presented next.

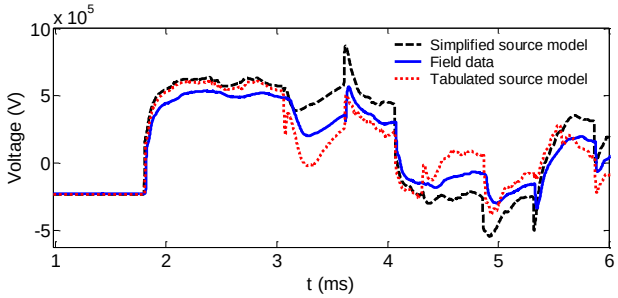

Fig. 7. Voltage of phase A at the Chemawa end, comparison between tabulated and simplified source model with the FD model.

V. Analysis of Line Parameters

The simplified source model, and the FD model are used to produce the simulation results of this section.

A. *Effect of the Parallel Lines*

The impact of parallel lines can be seen in Fig. 8 where simulation results are provided for the voltage of phase A at the Chemawa end for Case 5-03 with and without parallel lines. Removing the parallel lines reduces the simulated peak overvoltage from 4.63 pu to 3.65 pu. The results are non-intuitive, where the parallel line modeling further increases the overvoltages. The impact is mainly due to the closely-coupled 230 kV line. The impact of parallel lines on switching transients is discussed in many references including [18].

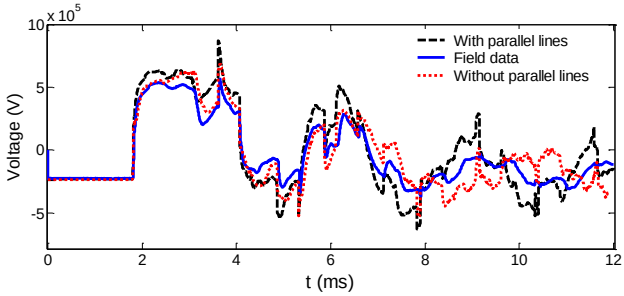

Fig. 8. Voltage of phase A at Chemawa end, effect of the parallel lines.

B. *Refinements in Ground Resistivity, Phase to Ground Conductance and Skin Effect Correction*

The BPA expert on transmission line ground resistivity estimated that the values would fall between 50 and 200 Ω-m, where the higher values might occur in mountainous regions [17]. Rather than using the default 100 Ω-m for the entire Big Eddy-Chemawa line, the following values are proposed [17]: i) 100 Ω-m for the first 23 miles (section 1), ii) 200 Ω-m for the next 38 miles (sections 2 to 4), and iii) 50 Ω-m for the remaining 55 miles (sections 5 to 9).

Considering possible additional losses in the line system, the assumed phase-to-ground conductance of 2e-10 S per unit length, is modified to 1e-8 S. Additionally, a correction on skin effect is considered by including the thickness-of-aluminum/outside diameter-of-conductor data [17]. The simulation results are shown in Fig. 9. The peak overvoltage reduces from 4.63 to 4.53 with the additional considerations in the computation of line parameters, and it is not possible to match field measurements through these refinements.

This article has been accepted for publication in a future issue of this journal, but has not been fully edited. Content may change prior to final publication. Citation information: DOI 10.1109/TPWRD.2018.2834138, IEEE Transactions on Power Delivery

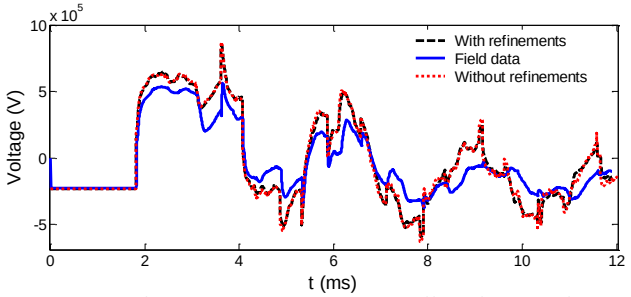

Fig. 9. Voltage of phase A at the Chemawa end, effect of model refinements.

C. *Detailed Source Model*

To obtain more precise results in the simulations, instead of the simplified source models described in section III-D, a detailed model is used to perform the switching transient analysis of case 5-03. The detailed system model includes all the surrounding elements in Fig. 1 with detailed parameters taken from [17].

The Big Eddy-Chemawa and the parallel lines are modeled as shown in Fig. 3, using the FD model for all the 10 sections. The trapped charge and the prestrike conditions are the same as described in Section III-B, and III-E, respectively. The simulated voltage of phase A at the Chemawa end is shown in Fig. 10. It is noticed that there is not a significant difference between the simulation results obtained with detailed and simplified source models.

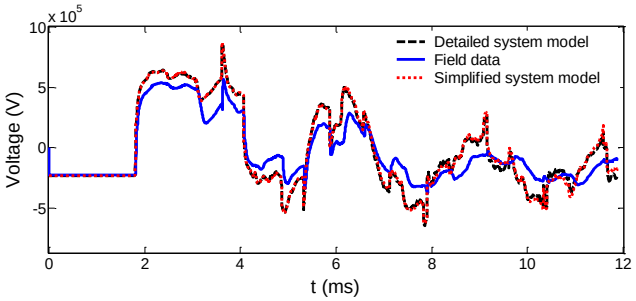

Fig. 10. Voltage of phase A at the Chemawa end considering a detailed source model.

D. *Discussion on Line Parameters*

Several different approaches have been considered to reproduce the field data for Case 5-03. Simulation results show that various improvements such as refinements in ground resistivity and phase-to-ground conductance, correction on skin effect and the use of detailed source model have little impact on the transient voltage waveform. This says that a phenomenon is present on the line that acts to reduce the switching surge magnitudes that hasn't yet been included. The effect of corona is considered next.

VI. Inclusion of the Corona Effect in the Line Model

Although considering the frequency dependence of line parameters without considering corona helped improve the simulation waveforms, it still overestimates the transients [11]-[15]. Corona has a strong effect on wave propagation [14].

In this paper, the Suliciu nonlinear corona model [13] and a linear model [16] are considered. The Suliciu model requires, in principle, the charge-voltage (Q-V) curve of the targeted transmission line, either obtained theoretically or by measurements. In addition, a specific EMT implementation is required for the solution of nonlinear equations and integration to the main solver of the EMT-type program [15].

The linear model is a piece-wise linear model of a nonlinear one and can be easily realized on any EMT-type simulation platform using basic components, i.e., resistors, capacitors and diodes. But the model produces spike-like voltages at the breaking points of the linear curves, like those of an arrester and a nonlinear inductor, as is well-known. The model components can be numerically evaluated by the user once the corona parameters specific to the targeted line are specified (corona onset voltage and corona loss constants) [16].

A. *Suliciu Corona Model*

For the inclusion of corona, the Big Eddy-Chemawa line, including the parallel lines, is divided into subsections of 0.6 miles long (approximately 1 km). The FD model is used for modeling each subsection. The Suliciu corona branch model [13] available in EMTP examples [15], is connected at each section as shown in Fig. 11.

The corona branch model equations are described in [13] and [15], and they are summarized in the appendix to define the corona parameters. The numerical values of the parameters used in this paper are also given in the appendix.

For the analysis of Case 5-03, the Big Eddy-Chemawa line is energized by: a) the tabulated source model as input source, and b) the simplified source model considering the prestrike conditions. Fig. 12 presents the voltage of phase A at the Chemawa end considering approaches a), and b). It can be observed in Fig. 12 that the simulation results are clearly better with the inclusion of corona. With the modeling approach a), a "*chopping*" condition is observed. The simplified source with prestrike modeling provides accurate results with a mismatch less than 0.01 pu in peak overvoltage (Fig. 12).

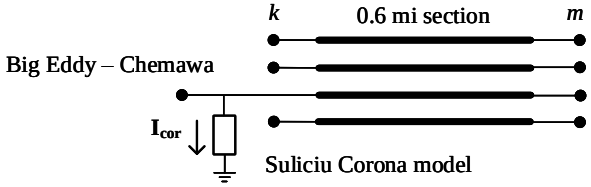

Fig. 11. Suliciu corona model (shunt branch) with FD model for each section.

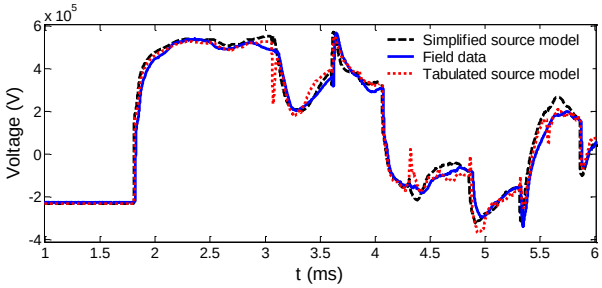

Fig. 12. Voltage of phase A at the Chemawa end with the Suliciu corona model.

This article has been accepted for publication in a future issue of this journal, but has not been fully edited. Content may change prior to final publication. Citation information: DOI 10.1109/TPWRD.2018.2834138, IEEE Transactions on Power Delivery

B. *Linear Corona Model*

The linear corona model described in [16] is also considered in this work. This model consists of a piecewise linear approximation. According to [16], three straight lines are sufficient to approximate the nonlinear characteristic of a nonlinear corona model. Thus, the model used in this paper includes three linear R-C parallel branches as detailed in the appendix. The constants of the linear corona model used in this paper are defined in the appendix together with the basic equations used to obtain them.

Considering that the Big Eddy-Chemawa line is energized by the simplified source model, the voltage of phase A at the Chemawa bus is shown in Fig. 13. The lines are divided into 0.6 miles long sections in both models to model the corona effect. It can be observed in Fig. 13 that there is no significant difference between the two corona models. But as the simulation time gets longer, the linear corona model presents spikes as seen in Fig. 14. Moreover, it requires careful tuning of the model parameters (corona onset voltages and loss constants) to match the pattern and peak. But, the Suliciu model is less sensitive to its parameters and it was even possible to obtain close results by using the example parameters for the 230-kV line in EMTP corona example.

The linear model was also tested in ATP by the WG members for Case 5-03 and the same results are obtained (not shown).

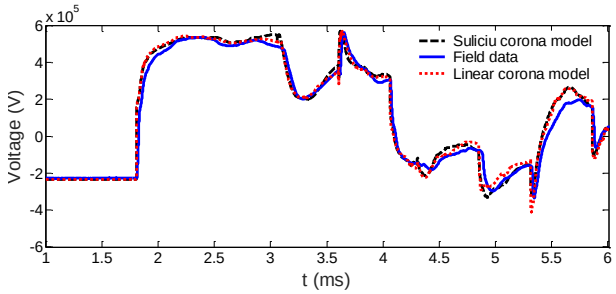

Fig. 13. Voltage of phase A at Chemawa end. Comparison of Sulicio and Linear Corona models.

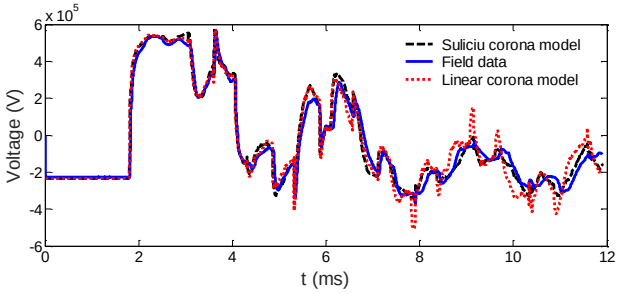

Fig. 14. Voltage of phase A at the Chemawa end. Comparison of the Suliciu and Linear Corona models. 12ms (high resolution field data).

C. *Longer Simulation Time*

Considering the simplified source model and the Suliciu corona model only, longer simulations were performed and compared with the field data. A 100 ms simulation is presented in Fig. 15 to show the steady-state solution after the switching transients have damped out. Fig. 15 shows that the simulation results match the field data with the inclusion of corona in the model and that the Suliciu corona model provides a stable steady-state result. The field data is available up to 66ms only.

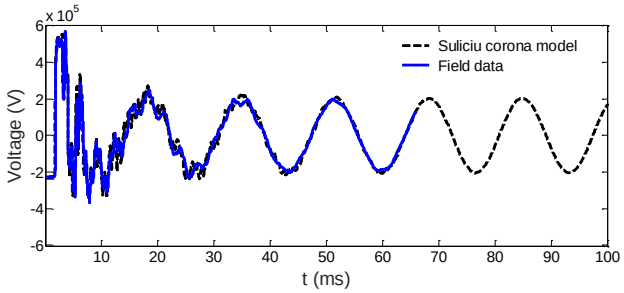

Fig. 15. Voltage of phase A at the Chemawa end including the Suliciu corona model for a 100 ms simulation time.

VII. Switching Transient Studies: Other Cases

This section studies four additional cases, i.e., Case 5-02, Case 5-05, Case 5-53 and Case 1-04. The relative energization angle, and the trapped charge values for the first three cases are already listed in Table II. The details for Case 1-04 is discussed below.

For the switching transient analysis of Case 5-02, Case 5-05, and Case 5-53, the test system of Fig. 1 is modeled as described in section III. The corona effect is included by dividing the Big Eddy-Chemawa line into sections of 0.6 mi, considering only the Suliciu model (with the parameters in Table VI). The Big Eddy-Chemawa line is energized by a simplified source model including the multiple prestrike conditions. For Case 5-02 and Case 5-05, the Big Eddy-Chemawa line is energized from the Big Eddy end (strong source), while for Case 5-53, it is energized from the Chemawa end (weak source). The switching times for all cases are shown in the Appendix. Fig. 16, Fig. 17, and Fig. 18 present simulation results for the cases 5-02, 5-05, and 5-53, respectively. In Fig. 16, the peak overvoltages are 2.69, 2.78 and 3.11 pu for measured, simulated with corona and without corona waveforms, respectively. With the same order, the overvoltages in Fig. 17 are 2.86, 2.97 and 3.41 pu while in Fig. 18 they are 2.65, 2.65 and 3.45 pu. It is observed that the match between simulation results and field measurements greatly improves with the inclusion of corona. In Fig. 18, phase C is shown as it presents the highest overvoltage.

Case 1-04 is a single-phase reclosing test performed on phase B. The trapped charges are -30.90, -171.9 and -23.23 kV for phases A, B and C respectively. The test system is modeled again as described in section III and the Big Eddy-Chemawa line is energized by a simplified source model. The single-pole closing time is 18.86 ms. As shown in Fig. 19, the peak overvoltages are 2.66, 2.65 and 2.97 pu respectively for measured and simulated waveforms with and without corona. Note that for a single-pole reclosing with trapped charge, the maximum expected overvoltage without considering corona is 3 pu, and the effect of corona is less important compared to three-phase cases.

It is also pointed out that for each three-phase switching case, one phase prestrikes first and creates a single-phase switching case until the induced surge from another phase reclosing reaches the line end. In most of the plots of this paper, the time between these events is more than a

This article has been accepted for publication in a future issue of this journal, but has not been fully edited. Content may change prior to final publication. Citation information: DOI 10.1109/TPWRD.2018.2834138, IEEE Transactions on Power Delivery

millisecond, and the single-phase surge has reached the line end and completed its reflection and resulting overvoltage.

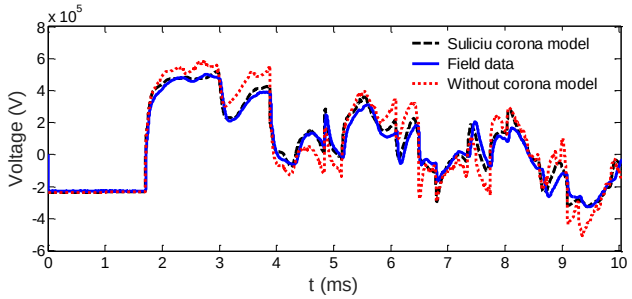

Fig. 16. Voltage of phase A at the Chemawa end. Case 5-02.

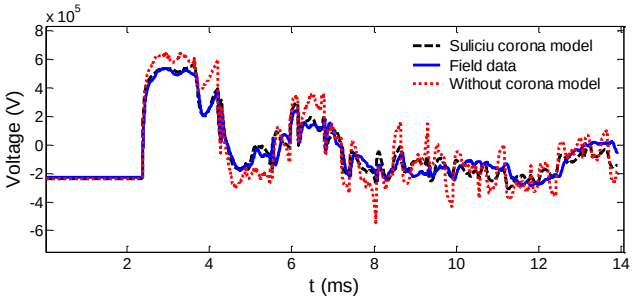

Fig. 17. Voltage of phase A at the Chemawa end. Case 5-05.

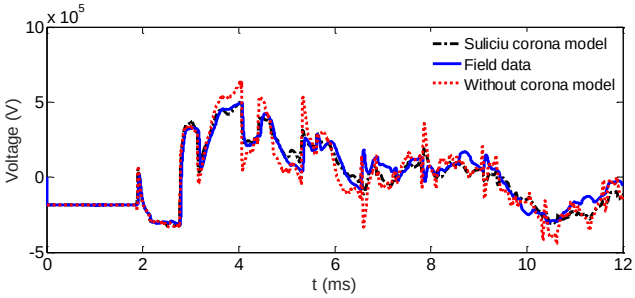

Fig. 18. Voltage of phase C at the Big Eddy end, Case 5-53.

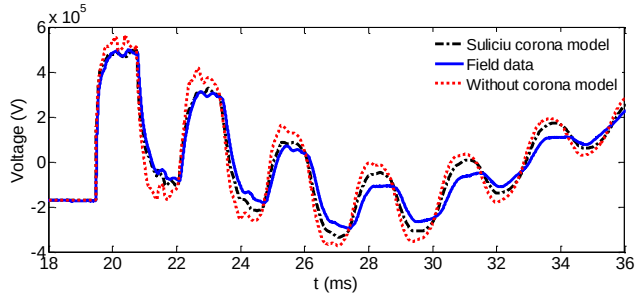

Fig. 19. Voltage of phase B at the Chemawa end, Case 1-04.

VIII. Conclusion

For transmission lines without switching surge mitigation, high-speed reclosing results in significant switching overvoltages due to the trapped charge on the line. With frequency-dependent line models and standard simulation techniques, the shapes of measured waveforms are reproduced well, but the peak overvoltages are considerably overestimated compared to actual field measurements. Variations in the numerous typical modeling parameters have shown to not solve the problem of higher simulated voltages. However, modeling corona on the switched line has proven to be the key for simulations to match the measurements. Corona, frequency dependence of line parameters and prestrike have been shown to be the most important factors in matching simulations to the field measured transients, both in terms of waveform pattern and magnitude, as presented here for a 230-kV line. This work provides the utility industry with a needed breakthrough in simulation techniques for performing switching surge studies and obtaining realistic results.

Appendix

A. Sequence of Switching Times

The sequence of switching times for Case 5-02, Case 5-03, Case 5-05 and Case 5-53 are shown in Table V.

TABLE V
Sequence of Switching Times

Phase	Condition	Time (ms)			
		Case 5-02	Case 5-03	Case 5-05	Case 5-53
A	Closes	0.000	0.000	0.000	0.000
	Opens	1.262	0.856	1.264	1.270
	Closes	2.180	2.260	1.832	2.170
	Opens	-	-	3.081	4.990
	Closes	-	-	3.575	5.380
B	Closes	5.087	4.060	3.776	3.730
	Opens	-	4.936	-	-
	Closes	-	6.100	-	-
C	Closes	3.130	1.800	1.894	0.890
	Opens	4.370	2.596	3.159	3.560
	Closes	4.780	3.510	4.140	4.660
	Opens	7.020	7.616	-	-
	Closes	7.380	8.510	-	-

B. Suliciu Model

Considering that x is the radius of a cylinder on which space charge is concentrated when conductor voltage falls to zero, then for a multiphase system:

$$\mathbf{V} = \mathbf{C_0^{-1}C_x V_x} + \mathbf{C_r^{-1}Q_c} \quad (1)$$

$$\mathbf{Q} = \mathbf{C_0 V} + \mathbf{C_0 C_x^{-1} Q_c} \quad (2)$$

where $\mathbf{V}$ is the line end (or section end) voltage, $\mathbf{V_x}$ is the voltage inside the cylinder, $\mathbf{Q}$ is the total line charge, $\mathbf{C_r}$ is the capacitance of the cylinder to ground, $\mathbf{C_x}$ is the capacitance of the line conductor to cylinder boundary, $\mathbf{Q_c}$ is the corona charge inside the cylinder and $\mathbf{C_0}$ is the geometric capacitance of the line [15]. Next, the corona charge is given by:

$$\mathbf{Q_{cor}} = \mathbf{C_0 C_x^{-1} Q_c} \quad (3)$$

and the corona branch current is found from:

$$\mathbf{I_{cor}} = \mathbf{C_0 C_x^{-1} I_c} \quad (4)$$

where $\mathbf{I_c}$ is the corona current vector inside the cylinder and its members can be found from the Suliciu equation [13]:

$$i_c = \frac{d}{dt} q_c = \begin{cases} 0 & \text{if } g_2 \le 0 \quad \text{state 6} \\ g_2 & \text{if } g_1 \le 0 < g_2 \quad \text{state 2} \\ g_1 + g_2 & \text{if } g_1 > 0 \quad \text{state 1} \end{cases} V_x > 0$$
$$\begin{cases} 0 & \text{if } g_4 \ge 0 \quad \text{state 5} \\ g_4 & \text{if } g_4 < 0 \le g_3 \quad \text{state 4} \\ g_3 + g_4 & \text{if } g_3 < 0 \quad \text{state 3} \end{cases} V_x \le 0 \quad (5)$$

$$g_j = k_j \left[(c_j - c_x)(v_x - v_j) - q_c \right] \quad j = 1 \text{K } 4$$

where k_j, c_j and v_j are model parameters, $c_x \in \mathbf{C_x}$, $v_x \in \mathbf{V_x}$ and $q_c \in \mathbf{Q_c}$. The Suliciu model parameters used in this paper are

given in Table VI. They are tuned by using the field measurements. Negative and positive sides of the Q-V curve are taken symmetrical and phase-to-phase corona is not considered.

TABLE VI
SULICIU MODEL PARAMETERS

Sections	1 - 4				5 - 9			
C_x (pF/m)	8.4				8			
	1	2	3	4	1	2	3	4
k (Hz)	1e5	0.1	1e5	0.1	1e5	0.1	1e5	0.1
c (pF/m)	22	35	22	35	30	35	30	35
v (kV)	400	230	-400	-230	380	230	-380	-230

C. The Linear Corona Model

The linear corona model used in this paper includes three linear R-C parallel branches as shown in Fig. 20. The parameters are computed as follows [16]:

$$V_1 = V_{co}, \quad V_2 = 2V_{co}, \quad V_3 = 3V_{co} \qquad (6a\text{-}c)$$

where V_{co} is the corona onset voltage in kV defined by

$$V_{co} = \frac{5nr}{3C}\left[1 + \frac{2r}{s}(n-1)\sin\left(\frac{\pi}{n}\right)\right] \qquad (7)$$

where C is the line charging capacitance in μF/km, n the number of bundles of a conductor, r the bundle radius in cm, and s the separation distance of the bundles in cm,

$$G_k = k_g\left[1 - \frac{V_{co}}{V_{co} + V_k}\right]^2 \Delta x, \quad C_k = 2k_g\left[1 - \frac{V_{co}}{V_{co} + V_k}\right]\Delta x \qquad (8\text{-}9)$$

where G_k is a linear conductance in S, C_k is a linear capacitance in F, V_k represents the DC voltage source (k=1,2,3), Δx is the separation distance of the corona models in m and,

$$k_g = \sigma_g\sqrt{\frac{a}{2h}}x10^{-11}, \quad k_c = \sigma_c\sqrt{\frac{a}{2h}}x10^{-11} \qquad (10\text{-}11)$$

where a is the conductor radius in m, h is the conductor height in m, σ_g and σ_c are the corona loss constants in S/m and F/m. The corona loss constants and onset voltages used in this paper are given in Table VII. They are obtained by using the field measurements. Only the positive side of the Q-V curve is considered as the overvoltages in this paper are on that side.

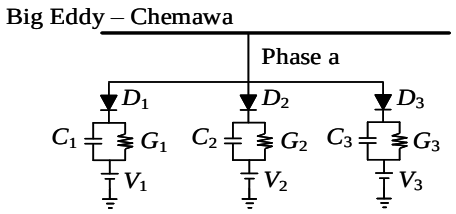

Fig. 20. Linear corona model of phase A inserted after each section.

TABLE VII
LINEAR CORONA MODEL PARAMETERS

Section	V_{co} (kV)	σ_g (10^6 S/m)	σ_c (F/m)
1	405	0.13	20.6
2-4	402	0.13	23
5-9	375	0.13	33

REFERENCES

[1] *IEEE Guide for the Application of Insulation Coordination*, IEEE Standard 1313.2–1999, 1999.

[2] A. Greenwood, *Electrical Transients in Power Systems*, 2 ed. New York, USA: Wiley, 1991.

[3] J.A. Martinez-Velasco, *Power System Transients. Parameter Determination*. Boca Raton, FL, USA: CRC Press, 2009.

[4] A. R. Hileman, P. R. Leblanc, and G. W. Brown, "Estimating the switching-surge performance of transmission lines," *IEEE Trans. Power App. Syst.*, vol. PAS-89, no. 7, pp. 1455–1469, Sep. 1970.

[5] D. A. Woodford and L. M. Wedepohl, "Impact of circuit breaker prestrike on transmission line energization transients," *Int. Conf. Power Syst. Transients*, Seattle, WA, USA, Jun. 1997.

[6] J. A. Martinez, D. Goldsworthy and R. Horton, "Switching Overvoltage Measurements and Simulations—Part I: Field Test Overvoltage Measurements," *IEEE Trans. on Power Del.*, vol. 29, no. 6, pp. 2502-2509, Dec. 2014.

[7] S.M. Lowder, J.L. Randall, and D. Goldsworthy, "Big Eddy-Chemawa 230-kV Line Switching and Transformer Saturation Test," Bonneville Power Administration, Report TTL(E) 96-11, June 7-8 1995.

[8] A. Morched, B. Gustavsen, and M. Tartibi, "A universal model for accurate calculation of electromagnetic transients on overhead lines and underground cables," *IEEE Trans. on Power Del.*, vol. 14, pp. 1032-1038, Jul 1999.

[9] J.R. Marti, "Accurate modeling of frequency-dependent transmission lines in electromagnetic transient simulations," *IEEE Trans. on Power Apparatus and Systems*, vol. 101, no. 1, pp. 147-155, January 1982.

[10] H. W. Dommel, *Electromagnetic Transients Program: Reference Manual: (EMTP Theory Book):* Bonneville Power Administration, 1986.

[11] C. Gary, G. Dragan and D. Critescu, "Attenuation of Travelling Waves Caused by Corona". CIGRE Report 33-13, 1978.

[12] C. Gary, A. Timotin and D. Critescu, "Prediction of Surge Propagation Influenced by Corona and Skin Effect". Proc. IEE, 130-A, pp. 264-272, July 1983.

[13] M.M. Suliciu and I. Suliciu, "A Rate Type Constitutive Equation for the Description of the Corona Effect", IEEE Trans., Vol. PAS-100, No. 8, pp. 3681-3685, August 1981.

[14] A. Semlyen and H. Wei-Gang, "Corona Modelling for the Calculation of Transients on Transmission Lines," *IEEE Power Engineering Review*, vol. PER-6, pp. 57-57, 1986.

[15] J. Mahseredjian, Support Routine for the EMTP Dynamic Corona Model. Rapport (IREQ-4534, décembre 1989.

[16] N. Nagaoka, H. Motoyama, and A. Ametani, "Lightning surge calculations including corona effects using a two-conductor model," *Electric Power Systems Research*, vol. 13, pp. 31-41, 08/ 1987.

[17] D. Goldsworthy, "Big Eddy - Chemawa Line & Source Modeling Data," *IEEE Working Group on Field Measured Overvoltages and Their Analysis*, Report, 2016.

[18] T. Ono, "Study on switching overvoltages in power systems," CRIEPI Report No. 121, Jan. 1985.